LETTER

Manifesting the connection between topological structures of quantum stationary coherent states and bundles of classical Lissajous orbits

To cite this article: Y. F. Chen *et al* 2018 *EPL* **122** 30002

A Letters Journal Exploring
the Frontiers of Physics

May 2018

EPL, **122** (2018) 30002 www.epljournal.org
doi: 10.1209/0295-5075/122/30002

Manifesting the connection between topological structures of quantum stationary coherent states and bundles of classical Lissajous orbits

Y. F. Chen[1(a)], Y. H. Hsieh[1], J. C. Tung[2], H. C. Liang[3] and K. F. Huang[1]

[1] *Department of Electrophysics, National Chiao Tung University - Hsinchu, Taiwan*
[2] *Molecular Chirality Research Center, Chiba University - Chiba, Japan*
[3] *Institute of Optoelectronic Science, National Taiwan Ocean University - Keelung, Taiwan*

received 20 April 2018; accepted in final form 2 June 2018
published online 27 June 2018

PACS 03.65.-w – Quantum mechanics
PACS 03.65.Vf – Phases: geometric; dynamic or topological

Abstract – Quantum stationary coherent states with spatial intensities localized on Lissajous orbits are theoretically explored by taking the inverse Fourier transform of the time-dependent coherent state. It is analytically verified that the stationary coherent state can be expressed as an integral of the Gaussian wave packet over the classical periodic orbit. With the derived integral, the phase singularities of the stationary coherent state can be precisely manifested from low-order to extremely high-order states. It is found that the phase singularities near the cross-point of the Lissajous orbits are generally arranged as rhombic vortex arrays. Finally, the stationary coherent states can be used as a basis to manifest the connection between topological structures of quantum eigenstates and bundles of classical Lissajous orbits.

Introduction. – It has been proven that the characteristics of the interference generally cause the wave functions to contain phase singularities [1]. The phase singularity of the wave function is usually called the vortex due to the feature that the probability current density swirls around the phase singularity [2]. Optical vortex beams have been broadly explored in a variety of scientific fields including optical manipulation, quantum information and communications, quantum entanglement, etc. [3–12]. Inspired by the development of optical vortex beams, the exploration of structured quantum waves with vortices becomes an emerging area of research [13–20]. Over the past decades, the salient quantum phenomena such as conductance fluctuations in mesoscopic semiconductor billiards [21,22], oscillations in photo-detachment cross-sections [23,24], and shell effects in metallic clusters [25,26] have been widely confirmed to be relevant to the classical periodic orbits. Therefore, the wave functions related to periodic orbits and the topological structure of their phase singularities deserve to be explored in depth for understanding the quantum and classical connections as well as the mesoscopic quantum phenomena.

The harmonic oscillator plays a unique linchpin in scientific areas as diverse as mechanics, acoustics, electromagnetics, optics, and quantum mechanics [27]. The two-dimensional (2D) anisotropic harmonic oscillator with commensurate frequencies ω_1/ω_2 is a well-known example of a classical superintegrable system [28]. The periodic orbits of the 2D commensurate harmonic oscillator, depending on ω_1/ω_2, are known as Bowditch curves or Lissajous figures which were investigated by Nathaniel Bowditch in 1815 [29], and later in more detail by Jules Antoine Lissajous in 1857 [30] who explored the relative frequencies of two tuning forks to make a far-reaching discussion of these curves. On the contrary, the quantum eigenmodes for different 2D harmonic oscillators are always the same to be solved as the Hermite-Gaussian (HG) modes with rectangular symmetry [31], regardless of what the value of ω_1/ω_2 happens to be.

Nowadays, the analogy between the paraxial wave equation for the spherical laser cavity and the Schrödinger equation for the 2D harmonic oscillator enables the HG eigenmodes to be experimentally observed from laser transverse modes [32–35]. In addition to HG modes, we have systematically generated the high-order transverse modes with spatial patterns localized on Lissajous curves

(a)E-mail: yfchen@cc.nctu.edu.tw

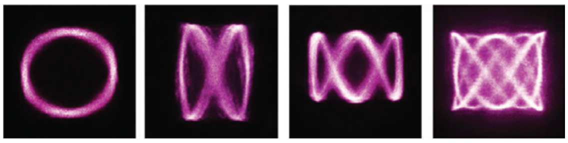

Fig. 1: (Colour online) Experimental observations for Lissajous modes emitted from a selectively end-pumped solid-state laser with astigmatism.

from a selectively end-pumped solid-state laser cavity with astigmatism [36,37], as shown in fig. 1 for some experimental results. Even though the $SU(2)$ coherent state has been theoretically exploited to reconstruct the experimental laser modes localized on Lissajous curves [36–38], this representation is a superposition of HG eigenmodes which cannot manifest the quantum-classical correspondence explicitly. It will be particularly interesting not only for quantum physics but also for laser physics to establish a complete relationship between quantum wave functions and classical periodic orbits in the 2D harmonic oscillator.

In this work, we take the inverse Fourier transform for the time-dependent coherent state of the 2D harmonic oscillator to derive the quantum Lissajous modes as an integral of the Gaussian wave packet over the classical Lissajous orbit. The derivation clearly reveals that the accidental degeneracies play an indispensable role in the formation of quantum wave functions concentrated on classical periodic orbits. More remarkably, the derived integral for representing the Lissajous modes can be used to express the probability current density straightforwardly without involving the HG eigenmodes. The calculated results for the probability current density not only confirm that the streamlines of probability current density along the classical trajectories coincide with the directions of classical velocities but also display the swirly feature of the probability flows around phase singularities. Furthermore, it is intriguingly found that the phase singularities near each crossing point of the Lissajous orbit generally exhibit a rhombic array of vortex lattice. Finally, we employ the quantum Fourier transform to verify that the HG eigenmode can be decomposed as a summation of generalized Lissajous modes with different phase factors. This decomposition clearly manifests the relationship between the topological structures of HG eigenmodes and the classical periodic orbits.

The integral formula for quantum stationary coherent states. – For the 2D commensurate harmonic oscillator, the Schrödinger equation is given by

$$\left[-\frac{\hbar^2}{2\mu}\left(\frac{\mathrm{d}^2}{\mathrm{d}\,x^2}+\frac{\mathrm{d}^2}{\mathrm{d}\,y^2}\right)+\frac{1}{2}\mu\,\left(\omega_1^2x^2+\omega_2^2y^2\right)\right]\psi(x,y)= E\psi(x,y), \tag{1}$$

where μ is the mass of the particle. For the frequency ratio ω_1/ω_2 to be a rational number q/p, where q and p are coprime integers, the characteristic frequencies can be written as $\omega_1 = q\omega$ and $\omega_2 = p\omega$. For isotropic harmonic oscillator $\omega_1/\omega_2 = 1$, the characteristic frequencies are given by $\omega_1 = \omega_2 = \omega$. In terms of the dimensionless variables, $\tilde{x} = \sqrt{\mu\omega_1/\hbar}\,x$ and $\tilde{y} = \sqrt{\mu\omega_2/\hbar}\,y$, the eigenfunction can be expressed as the product of two separate eigenfunctions of 1D harmonic oscillator, *i.e.*,

$$\psi^{(HG)}_{n_1,n_2}(\tilde{x},\tilde{y}) = \psi_{n_1}(\tilde{x})\psi_{n_2}(\tilde{y}), \tag{2}$$

where

$$\psi_n(\xi) = \frac{1}{\sqrt{2^n n\,!\sqrt{\pi}}}H_n(\xi)\,e^{-\xi^2/2}, \tag{3}$$

and $H_n(\cdot)$ are the Hermite polynomials of order n. The eigenvalue for $\psi^{(HG)}_{n_1,n_2}(\tilde{x},\tilde{y})$ is given by

$$\omega_{n_1,n_2} = E_{n_1,n_2}/\hbar = (n_1q+n_2p)\,\omega + \frac{(p+q)}{2}\omega. \tag{4}$$

In terms of a complex variable τ, the generating function for the Hermite polynomials is generally given by [30]

$$e^{-\tau^2+2\tau\,\xi} = \sum_{n=0}^{\infty}\frac{\tau^n}{n\,!}H_n(\xi). \tag{5}$$

Setting $\tau = u/\sqrt{2}$ and multiplying the term $e^{-(|u|^2+\xi^2)/2}$ on the both sides of eq. (5), after some rearrangement and in terms of $\psi_n(\tilde{x})$, the generating function can be used to express the Gaussian wave packet as

$$\pi^{-1/4}\,e^{-(\xi^2-2\sqrt{2}u\,\xi+u^2+|u|^2)/2} = \sum_{n=0}^{\infty}\frac{u^n}{\sqrt{n\,!}}e^{-|u|^2/2}\;\psi_n(\xi). \tag{6}$$

Equation (6) was originally derived by Schrödinger for manifesting the quantum-classical connection of the 1D harmonic oscillator. Applying eq. (6) to the 2D harmonic oscillator, the time-dependent coherent state can be expressed as

$$\begin{aligned} &g(\tilde{x},\tilde{y},u_1,u_2) = \\ &\frac{1}{\sqrt{\pi}}e^{-\frac{(\tilde{x}^2-2\sqrt{2}u_1\tilde{x}+u_1^2+|u_1|^2)}{2}}e^{-\frac{(\tilde{y}^2-2\sqrt{2}u_2\,\tilde{y}+u_2^2+|u_2|^2)}{2}} \\ &= \sum_{n_1=0}^{\infty}\sum_{n_2=0}^{\infty}\frac{u_1^{n_1}}{\sqrt{n_1\,!}}\frac{u_2^{n_2}}{\sqrt{n_2\,!}}e^{-\frac{|u_1|^2+|u_2|^2}{2}}\;\psi^{(HG)}_{n_1,n_2}(\tilde{x},\tilde{y}), \end{aligned} \tag{7}$$

where $u_1 = \sqrt{N_1}e^{-i[q(\omega t+\phi_1)]}$, $u_2 = \sqrt{N_2}e^{-i[p(\omega t+\phi_2)]}$, N_1 and N_2 are related to the oscillation amplitude, and ϕ_1 and ϕ_2 are related to the initial position. Clearly, the intensity $|g(\tilde{x},\tilde{y},u_1,u_2)|^2$ represents a Gaussian wave packet with the central peak to mimic the classical trajectory $\tilde{x} = \sqrt{2}\mathrm{Re}(u_1) = \sqrt{2N_1}\cos[q(\omega t+\phi_1)]$ and $\tilde{y} = \sqrt{2}\mathrm{Re}(u_2) = \sqrt{2N_2}\cos[p(\omega t+\phi_2)]$.

Since the structure of the classical orbit depends only on the relative phase between ϕ_1 and ϕ_2, the parameters u_1 and u_2 are conveniently expressed as

$$\begin{bmatrix} u_1 \\ u_2 \end{bmatrix} = \begin{bmatrix} \sqrt{N_1}\;e^{-i[q(\theta+\phi/2)]} \\ \sqrt{N_2}\;e^{-i[p(\theta-\phi/2)]} \end{bmatrix}, \tag{8}$$

where the variable θ stands for ωt to cover the range from 0 to 2π for a complete orbit and the phase factor ϕ determines the trajectorial structure. Substituting eq. (8) into eq. (7), the summation terms for the wave packet $g(\tilde{x},\tilde{y},u_1,u_2)$ can be rearranged as

$$\begin{aligned} & g(\tilde{x},\tilde{y},u_1,u_2) = \\ & \frac{1}{\sqrt{\pi}} e^{-\frac{(\tilde{x}^2-2\sqrt{2}u_1\tilde{x}+u_1^2+|u_1|^2)}{2}} e^{-\frac{(\tilde{y}^2-2\sqrt{2}u_2\tilde{y}+u_2^2+|u_2|^2)}{2}} \\ & = \sum_{n_1=0}^{\infty}\sum_{n_2=0}^{\infty} \frac{N_1^{n_1/2}}{\sqrt{n_1!}}\frac{N_2^{n_2/2}}{\sqrt{n_2!}} e^{-\frac{N_1+N_2}{2}} \psi_{n_1,n_2}^{(HG)}(\tilde{x},\tilde{y}) \\ & \cdot e^{-i(qn_1+pn_2)\theta}\, e^{-i(qn_1-pn_2)\phi/2}. \end{aligned} \tag{9}$$

As seen in eq. (4), the differences of eigenvalues utterly arise from the term qn_1+pn_2. In other words, for a given (N_1,N_2) the eigenstates $\psi_{n_1,n_2}^{(HG)}(\tilde{x},\tilde{y})$ satisfying the equation of $qn_1+pn_2=qN_1+pN_2$ are degenerate. As a consequence, the time-dependent wave packet $g(\tilde{x},\tilde{y},u_1,u_2)$ in eq. (9) can be expressed as the superposition of the stationary coherent states that have the eigenvalues to correspond to the term qn_1+pn_2. The kernel of the inverse Fourier transform

$$\frac{1}{2\pi}\int_0^{2\pi} e^{i(n-n')\theta}\mathrm{d}\theta = \delta_{n,n'} \tag{10}$$

can be applied to eq. (9) to derive the stationary coherent state from the integral

$$\Psi_{N_1,N_2}^{(q,p)}(\tilde{x},\tilde{y},\phi) = \frac{1}{2\pi}\int_0^{2\pi} g(\tilde{x},\tilde{y},u_1,u_2)\, e^{i\,(qN_1+pN_2)\theta}\mathrm{d}\theta. \tag{11}$$

It can be simply confirmed that the group of degenerate eigenstates $\psi_{n_1,n_2}^{(HG)}(\tilde{x},\tilde{y})$ for a given (N_1,N_2) can be specified as $n_1=N_1-pK$ and $n_2=N_2+qK$, where K is an arbitrary integer. Consequently, the stationary coherent state in eq. (11) can be derived as

$$\begin{aligned} & \Psi_{N_1,N_2}^{(q,p)}(\tilde{x},\tilde{y},\phi) = \\ & \frac{1}{2\pi}\int_0^{2\pi} \frac{1}{\sqrt{\pi}} e^{-\frac{(\tilde{x}^2-2\sqrt{2}u_1\tilde{x}+u_1^2+|u_1|^2)}{2}} e^{-\frac{(\tilde{y}^2-2\sqrt{2}u_2\tilde{y}+u_2^2+|u_2|^2)}{2}} \\ & \cdot e^{i\,(qN_1+pN_2)\theta}\mathrm{d}\theta = \\ & \sum_{K=-[N_2/q]}^{[N_1/p]} \frac{N_1^{(N_1-pK)/2}}{\sqrt{(N_1-pK)!}}\frac{N_2^{(N_2+qK)/2}}{\sqrt{(N_2+qK)!}} e^{-\frac{N_1+N_2}{2}} \\ & \cdot e^{-i(qN_1-pN_2)\,\phi/2}\psi_{N_1-pK,N_2+qK}^{(HG)}(\tilde{x},\tilde{y})\, e^{i\,K\,q\,p\,\phi}. \end{aligned} \tag{12}$$

For a given (N_1,N_2,ϕ), the total number of the degenerate eigenstates $\psi_{N_1-pK,N_2+qK}^{(HG)}(\tilde{x},\tilde{y})$ is given by $M=[N_1/p]+[N_2/q]+1$. As long as $M\gg 1$,the spatial intensities of the stationary coherent states $\Psi_{N_1,N_2}^{(q,p)}(\tilde{x},\tilde{y},\phi)$ are exactly concentrated on the Lissajous figures. The summation expression in eq. (12) is exactly the same as the representation of the $SU(2)$ coherent state [38–43] that has been used to analyze the quantum wave function corresponding to Lissajous figure. Here it is verified that

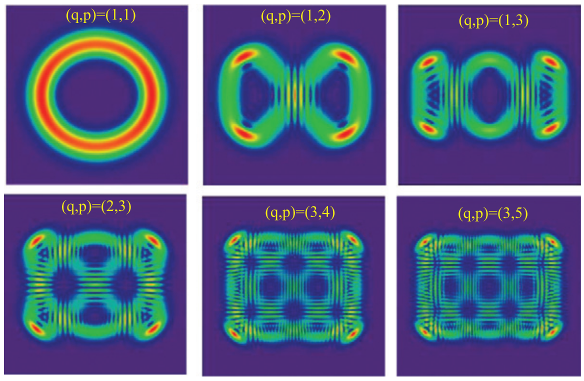

Fig. 2: (Colour online) Numerical results of the wave patterns $|\Psi_{N_1,N_2}^{(q,p)}(\tilde{x},\tilde{y},\phi)|$ for six different (q,p) with $N_1=8p$, $N_2=7q$, and $q\,p\,\phi=\pi/2$.

the Lissajous mode $\Psi_{N_1,N_2}^{(q,p)}(\tilde{x},\tilde{y},\phi)$ can be expressed as an integral of the Gaussian wave-packet state over the Lissajous orbit. More remarkably, the integral expression in eq. (12) not only transparently manifests the quantum-classical correspondence but also can be straightforwardly calculated without involving the computation of eigenmodes $\psi_{N_1-pK,N_2+qK}^{(HG)}(\tilde{x},\tilde{y})$. Figure 2 shows the numerical results of the wave patterns $|\Psi_{N_1,N_2}^{(q,p)}(\tilde{x},\tilde{y},\phi)|$ for six different (q,p) with $N_1=8p$, $N_2=7q$, and $q\,p\,\phi=\pi/2$. The calculated wave patterns can be clearly seen to be exactly in agreement with Lissajous orbits. On the other hand, when the indices (N_1,N_2) are so small that $N_1<p$ and $N_2<q$, there are no degenerate eigenstates in the stationary coherent state $\Psi_{N_1,N_2}^{(q,p)}(\tilde{x},\tilde{y},\phi)$. Under this circumstance, the stationary coherent state $\Psi_{N_1,N_2}^{(q,p)}(\tilde{x},\tilde{y},\phi)$ is just the pure single eigenstate $\psi_{N_1,N_2}^{(HG)}(\tilde{x},\tilde{y})$ and its wave pattern is independent of the relative phase factor ϕ.

The probability current density for a wave function $\Psi(\tilde{x},\tilde{y})$ is given by

$$\mathbf{J}(\tilde{x},\tilde{y}) = \frac{\hbar}{\mu}\mathrm{Im}\left[\Psi^*(\tilde{x},\tilde{y})\nabla\Psi(\tilde{x},\tilde{y})\right]. \tag{13}$$

For the stationary coherent state $\Psi_{N_1,N_2}^{(q,p)}(\tilde{x},\tilde{y},\phi)$, the integral form in eq. (11) can be used to obtain

$$\begin{aligned} & \nabla\Psi_{N_1,N_2}^{(q,p)}(\tilde{x},\tilde{y},\phi) = \\ & \frac{-1}{2\pi}\int_0^{2\pi} g(\tilde{x},\tilde{y},u_1,u_2)\left[\mathbf{a}_x(\tilde{x}-\sqrt{2}u_1)+\mathbf{a}_y(\tilde{y}-\sqrt{2}u_2)\right] \\ & \cdot e^{i\,(qN_1+pN_2)\theta}\mathrm{d}\theta. \end{aligned} \tag{14}$$

By using eqs. (11) and (14), the probability current density $\mathbf{J}(\tilde{x},\tilde{y})$ for the stationary coherent state $\Psi_{N_1,N_2}^{(q,p)}(\tilde{x},\tilde{y},\phi)$ can be straightforwardly calculated without using the eigenmodes $\psi_{N_1-pK,N_2+qK}^{(HG)}(\tilde{x},\tilde{y})$. Figure 3 shows the numerical results of the probability current density $\mathbf{J}(\tilde{x},\tilde{y})$ for the stationary coherent state $\Psi_{N_1,N_2}^{(q,p)}(\tilde{x},\tilde{y},\phi)$ displayed in fig. 2. The streamlines of probability flows along the

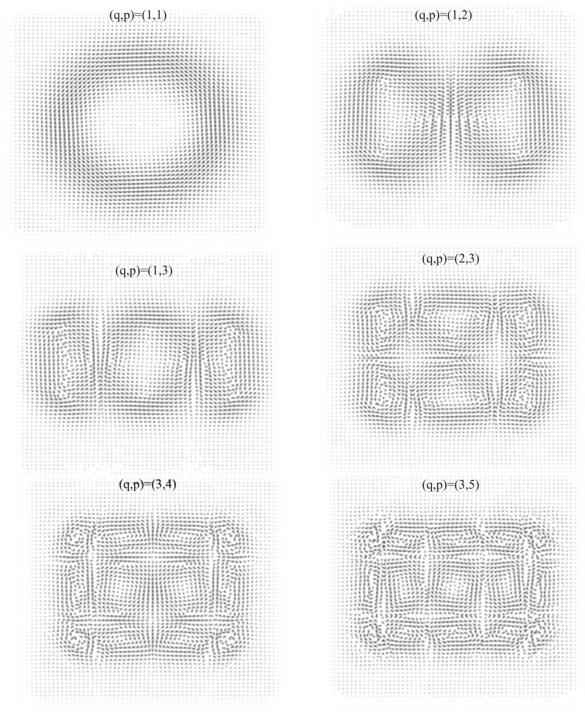

Fig. 3: (Colour online) Numerical results of the probability current density $\mathbf{J}(\tilde{x},\tilde{y})$ for the stationary coherent state $\Psi^{(q,p)}_{N_1,N_2}(\tilde{x},\tilde{y},\phi)$ displayed in fig. 2.

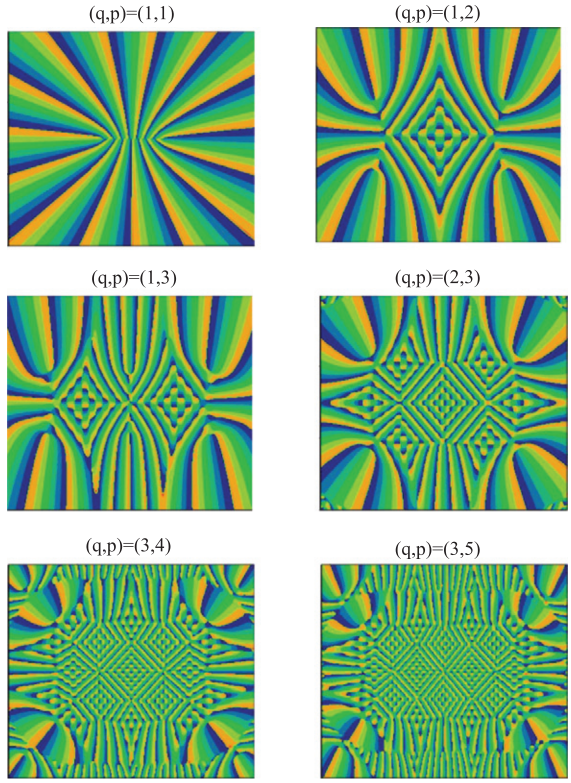

Fig. 4: (Colour online) Numerical results of the phase distribution $\Theta(\tilde{x},\tilde{y})$ for the probability current density $\mathbf{J}(\tilde{x},\tilde{y})$ shown in fig. 3.

classical trajectories can be seen to consist with the directions of classical velocities. On the contrary, the swirly feature of the probability current density around the phase singularity is a distinctly non-classical character of quantum structured wave. The structure of the phase singularities can be manifested by the phase distribution of the wave function that is given by

$$\Theta(\tilde{x},\tilde{y}) = \tan^{-1}\left\{\frac{\mathrm{Im}\left[\Psi^{(q,p)}_{N_1,N_2}(\tilde{x},\tilde{y},\phi)\right]}{\mathrm{Re}\left[\Psi^{(q,p)}_{N_1,N_2}(\tilde{x},\tilde{y},\phi)\right]}\right\}. \qquad (15)$$

The relationship between $\Theta(\tilde{x},\tilde{y})$ and $\mathbf{J}(\tilde{x},\tilde{y})$ is given by

$$\mathbf{J}(\tilde{x},\tilde{y}) = \frac{\hbar}{\mu}\rho(\tilde{x},\tilde{y})\,\nabla\Theta(\tilde{x},\tilde{y}), \qquad (16)$$

where $\rho(\tilde{x},\tilde{y}) = |\Psi^{(q,p)}_{N_1,N_2}(\tilde{x},\tilde{y},\phi)|^2$. Figure 4 depicts the numerical results of the phase distribution $\Theta(\tilde{x},\tilde{y})$ for the probability current density $\mathbf{J}(\tilde{x},\tilde{y})$ shown in fig. 3. Note that the Lissajous orbit always intersects itself except for the case $(q,p) = (1,1)$. From fig. 4, the phase structure near the crossing point can be seen to display an array of isolated singularities that are arranged in the rhombic shape.

Decomposition of eigenmodes based on stationary coherent states. – The discrete Fourier transform $\{F_0,\ F_1,\cdots,F_{M-1}\}$ of a discrete function $\{f_0,\ f_1,\cdots,f_{M-1}\}$ and its inverse are given by

$$F_k = \frac{1}{M}\sum_{m=0}^{M-1} f_m\, e^{-i2\pi m\, k/M}, \qquad (17)$$

$$f_m = \sum_{k=0}^{M-1} F_k\, e^{i2\pi m\, k/M}. \qquad (18)$$

The quantum Fourier transform is a discrete Fourier transform upon the quantum state. From eq. (12), it can be found that the stationary coherent state $\Psi^{(q,p)}_{N_1,N_2}(\tilde{x},\tilde{y},\phi)$ consists of $M = [N_1/p] + [N_2/q] + 1$ degenerate eigenmodes $\psi^{(HG)}_{N_1-pK,N_2+qK}(\tilde{x},\tilde{y})$ with the weighting coefficient including the relative phase term $e^{i\,K\,q\,p\,\phi}$. We can use the concept of the discrete Fourier transform to divide the phase factor ϕ into M different values given by $q\,p\,\phi_m = 2\pi m/M$ with $m = 0,1,\cdots,M-1$. Consequently, the set $\{\Psi^{(q,p)}_{N_1,N_2}(\tilde{x},\tilde{y},\phi_m)\}$ can form a complete basis to represent the eigenmode $\psi^{(HG)}_{N_1-pK,N_2+qK}(\tilde{x},\tilde{y})$ by means of the inverse quantum Fourier transform. The inverse Fourier transform for eq. (12) can be derived as

$$\frac{N_1^{(N_1-pK)/2}}{\sqrt{(N_1-pK)\,!}}\frac{N_2^{(N_2+qK)/2}}{\sqrt{(N_2+qK)\,!}}e^{-\frac{N_1+N_2}{2}}\psi^{(HG)}_{N_1-pK,N_2+qK}(\tilde{x},\tilde{y}) = \frac{1}{M}\sum_{m=0}^{M-1}\Psi^{(q,p)}_{N_1,N_2}(\tilde{x},\tilde{y},\phi_m)\,e^{i(qN_1-pN_2)\,\phi_m/2}e^{-iKqp\,\phi_m}, \qquad (19)$$

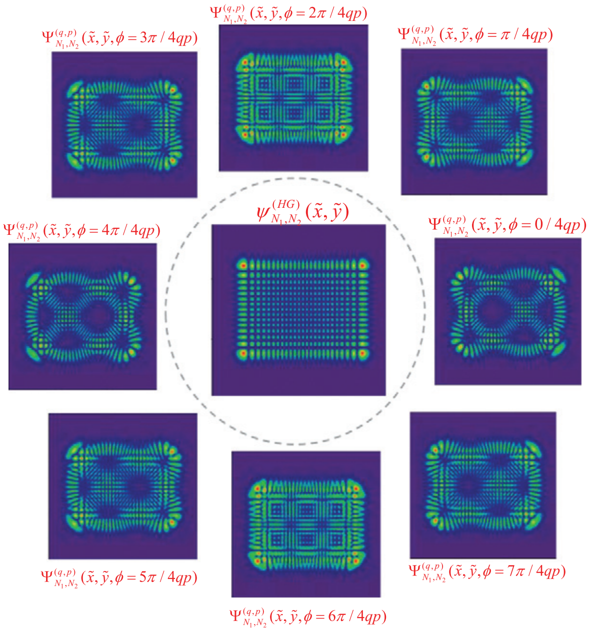

Fig. 5: (Colour online) Calculated results for $\psi^{(HG)}_{N_1,N_2}(\tilde{x},\tilde{y})$ and $\Psi^{(q,p)}_{N_1,N_2}(\tilde{x},\tilde{y},\phi_m)$ by using eqs. (12) and (20) for $(N_1,N_2) = (24,14)$ and $(q,p)=(4,5)$.

where the index K is the integer between $K = -[N_2/q]$ and $K = [N_1/p]$. No matter what the numbers N_1 and N_2 are, eq. (19) is definitely available for $K = 0$. Substituting $K = 0$ into eq. (19), the eigenmode $\psi^{(HG)}_{N_1,N_2}(\tilde{x},\tilde{y})$ can be derived as

$$\psi^{(HG)}_{N_1,N_2}(\tilde{x},\tilde{y}) = C_{N_1,N_2}\frac{1}{M}\sum_{m=0}^{M-1}\Psi^{(q,p)}_{N_1,N_2}(\tilde{x},\tilde{y},\phi_m) \times e^{\,i(qN_1-pN_2)\,\phi_m/2}, \tag{20}$$

where

$$C_{N_1,N_2} = \left[\frac{N_1^{N_1/2}}{\sqrt{N_1\,!}}\frac{N_2^{N_2/2}}{\sqrt{N_2\,!}}e^{-\frac{N_1+N_2}{2}}\right]^{-1}, \tag{21}$$

The expression in eq. (20) reveals that the eigenmode $\psi^{(HG)}_{N_1,N_2}(\tilde{x},\tilde{y})$ can be considered as a summation of M generalized Lissajous modes $\Psi^{(q,p)}_{N_1,N_2}(\tilde{x},\tilde{y},\phi_m)$, where each Lissajous mode exactly ono-to-one corresponds to a classical orbit. Moreover, eq. (20) provides a general expression for the eigenmode $\psi^{(HG)}_{N_1,N_2}(\tilde{x},\tilde{y})$ without involving the Hermite polynomials. Since the number M is given by $M = [N_1/p] + [N_2/q] + 1$, its value depends (q,p) for a fixed (N_1,N_2). In other words, the same eigenmode $\psi^{(HG)}_{N_1,N_2}(\tilde{x},\tilde{y})$ can be decomposed as different Lissajous modes, depending on (q,p). Considering $(N_1,N_2) = (24,14)$ as an example, the value of M can be found to be 8 for $(q,p) = (4,5)$ and 16 for $(q,p) = (2,3)$. Figure 5 shows the calculated results for $\psi^{(HG)}_{N_1,N_2}(\tilde{x},\tilde{y})$ and $\Psi^{(q,p)}_{N_1,N_2}(\tilde{x},\tilde{y},\phi_m)$ by using eqs. (12) and (20) for $(N_1,N_2) = (24,14)$ and $(q,p) = (4,5)$, where the values for

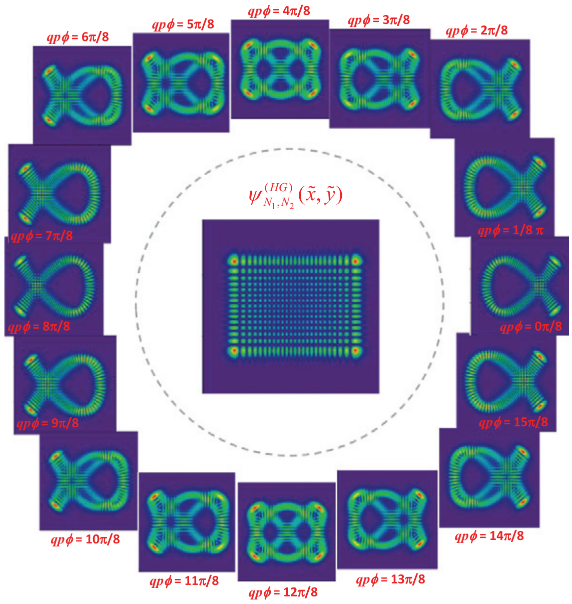

Fig. 6: (Colour online) A plot similar to fig. 5 for the case of $(N_1,N_2) = (24,14)$ and $(q,p) = (2,3)$.

ϕ_m are given by $\phi_m = 2\pi m/8q\,p$ with $m = 0,1,\cdots,7$. The relationship between $\psi^{(HG)}_{N_1,N_2}(\tilde{x},\tilde{y})$ and $\Psi^{(q,p)}_{N_1,N_2}(\tilde{x},\tilde{y},\phi_m)$ can be clearly seen. Figure 6 shows a similar plot for the case of $(N_1,N_2) = (24,14)$ and $(q,p) = (2,3)$, where the values for ϕ_m are given by $q\,p\,\phi_m = 2\pi m/16$ with $m = 0,1,\cdots,15$. Compared with the results shown in fig. 5 for the same $(N_1,N_2) = (24,14)$, the number of superposed Lissajous modes in fig. 6 becomes more due to smaller values for (q,p).

Conclusions. – In conclusion, structured quantum waves related to Lissajous curves have been analytically derived as an integral of the Gaussian wave packet over the classical periodic orbit by taking the inverse Fourier transform for the time-dependent coherent state of the 2D harmonic oscillator. The derived integral for expressing quantum Lissajous modes can be straightforwardly used to analyze the probability current density to explore the phase structure without involving the HG eigenmodes. The calculated results for the probability current density reveal that the streamlines of probability current density along the classical trajectories coincide with the directions of classical velocities. More intriguingly, the phase singularities near the cross-point of the Lissajous curve are found to generally exhibit a rhombic vortex array. By means of quantum Fourier transform, the generalized Lissajous modes have been employed to decompose the HG eigenmode for understanding the relationship between the topological structures of eigenmodes and the classical periodic orbits.

* * *

This work is supported by the Ministry of Science and Technology of Taiwan (Contract No. 106-2628-M-009-001).

REFERENCES

[1] Masajada J. and Dubik B., *Opt. Commun.*, **198** (2001) 21.

[2] Soskin M. S. and Vasnetsov M. V., *Prog. Opt.*, **42** (2001) 219.

[3] Indebetouw G., *J. Mod. Opt.*, **40** (1993) 73.

[4] Andrews D. L., *Structured Light and Its Applications: An Introduction to Phase-Structured Beams and Nanoscale Optical Force* (Academic Press, New York) 2008.

[5] Santamato E., Sasso A., Piccirillo B. and Vella A., *Opt. Express*, **10** (2002) 871.

[6] Gahagan K. T. and Swartzlander G. A. jr., *Opt. Lett.*, **21** (1996) 827.

[7] MacDonald M. P., *Opt. Commun.*, **201** (2002) 21.

[8] Song Y., Milam D. and Hill W. T., *Opt. Lett.*, **24** (1999) 1805.

[9] Xu X., Kim K., Jhe W. and Kwon N., *Phys. Rev. A*, **63** (2001) 3401.

[10] Kuga T., Torii Y., Shiokawa N., Hirano T., Shimizu Y. and Sasada H., *Phys. Rev. Lett.*, **78** (1997) 4713.

[11] Courtial J., Dholakia K., Robertson D. A., Allen L. and Padgett M. J., *Phys. Rev. Lett.*, **80** (1998) 013601.

[12] Mair A., Vaziri A., Weihs G. and Zeilinger A., *Nature*, **412** (2001) 313.

[13] Bialynicki-Birula I., Bialynicka-Birula Z. and Sliwa C., *Phys. Rev. A*, **61** (2000) 032110.

[14] Allen L. J., Faulkner H. M. L., Oxley M. P. and Paganin D., *Ultramicroscopy*, **88** (2001) 85.

[15] Bliokh K. Y., Bliokh Y. P., Savel'ev S. and Nori F., *Phys. Rev. Lett.*, **99** (2007) 190404.

[16] Uchida M. and Tonomura A., *Nature*, **464** (2010) 737.

[17] Verbeeck J., Tian H. and Schattschneider P., *Nature*, **467** (2010) 301.

[18] McMorran B. J., Agrawal A., Anderson I. M., Herzing A. A., Lezec H. J., McClelland J. J. and Unguris J., *Science*, **331** (2011) 192.

[19] Harris J., Grillo V., Mafakheri E., Gazzadi G. C., Frabboni S., Boyd R. W. and Karimi E., *Nat. Phys.*, **11** (2015) 629.

[20] Bliokh K. Y., Ivanov I. P., Guzzinati G., Clark L., Van Boxem R., Béché A., Juchtmans R., Alonso M. A., Schattschneider P., Nori F. and Verbeeck J., *Phys. Rep.*, **690** (2017) 1.

[21] Zozoulenko I. V. and Berggren K. F., *Phys. Rev. B*, **56** (1997) 6931.

[22] Brunner R., Meisels R., Kuchar F., Akis R., Ferry D. K. and Bird J. P., *Phys. Rev. Lett.*, **98** (2007) 204101.

[23] Peters A. D., Jaffé C. and Delos J. B., *Phys. Rev. Lett.*, **73** (1994) 2825.

[24] Bracher C. and Delos J. B., *Phys. Rev. Lett.*, **96** (2006) 100404.

[25] Brack M., *Rev. Mod. Phys.*, **65** (1993) 677.

[26] De Heer W. A., *Rev. Mod. Phys.*, **65** (1993) 611.

[27] Bloch S. C., *Introduction to Classic and Quantum Harmonic Oscillators* (Wiley-Blackwell, New York) 1997.

[28] Hietarinta J., *Phys. Rep.*, **147** (1987) 87.

[29] Bowditch N., *Mem. Am. Acad. Arts Sci.*, **3** (1815) 413.

[30] Lissajous J., *Ann. Chim. Phys.*, **51** (1857) 147.

[31] Flügge S., *Practical Quantum Mechanics* (Springer-Verlag, New York) 1971, p. 107.

[32] Chen Y. F., Huang T. M., Kao C. F., Wang C. L. and Wang S. C., *IEEE J. Quantum Electron.*, **33** (1997) 1025.

[33] Laabs H. and Ozygus B., *Opt. Laser Technol.*, **28** (1996) 213.

[34] Chen Y. F., Chang C. C., Lee C. Y., Sung C. L., Tung J. C., Su K. W., Liang H. C., Chen W. D. and Zhang G., *Photon. Res.*, **5** (2017) 561.

[35] Chen Y. F., Chang C. C., Lee C. Y., Tung J. C., Liang H. C. and Huang K. F., *Laser Phys.*, **28** (2018) 015002.

[36] Chen Y. F., Lu T. H., Su K. W. and Huang K. F., *Phys. Rev. Lett.*, **96** (2006) 213902.

[37] Tung J. C., Tuan P. H., Liang H. C., Huang K. F. and Chen Y. F., *Phys. Rev. A*, **94** (2016) 023811.

[38] Chen Y. F., *Phys. Rev. A*, **83** (2011) 032124.

[39] Górska K. J., Makowski A. J. and Dembiński S. T., *J. Phys. A*, **39** (2006) 13285.

[40] Pollet J., Méplan O. and Gignoux C., *J. Phys. A*, **28** (1995) 7282.

[41] Banerji J. and Agarwal G. S., *Opt. Express*, **5** (1999) 220.

[42] Xin J. and Liang J. Q., *Phys. Scr.*, **90** (2015) 065207.

[43] Kumar M. S. and Dutta-Roy B., *J. Phys. A*, **41** (2008) 075306.